Electronic Supplementary Information for

Rapid structural discrimination of IgG antibodies by multicharge-state collision-induced unfolding

Zhibin Yin [a], Mingyi Du [a,b], Dong Chen [a,b], Wenyang Zhang [a], Wenjie Huang [a], Xinzhou Wu [b,*], and Shijuan Yan [a,*]

[a] Guangdong Key Laboratory for Crop Germplasm Resources Preservation and Utilization, Agro-biological Gene Research Center, Guangdong Academy of Agricultural Sciences, Guangzhou, 510640, China

[b] State Key Laboratory for Conservation and Utilization of Subtropical Agro-bioresources and Key Laboratory of Natural Pesticide and Chemical Biology of the Ministry of Education, South China Agricultural University, Guangzhou, 510642, China

* E-mail addresses: wuxz@scau.edu.cn (X. Wu), shijuan@agrogene.ac.cn (S. Yan)

Table of Content

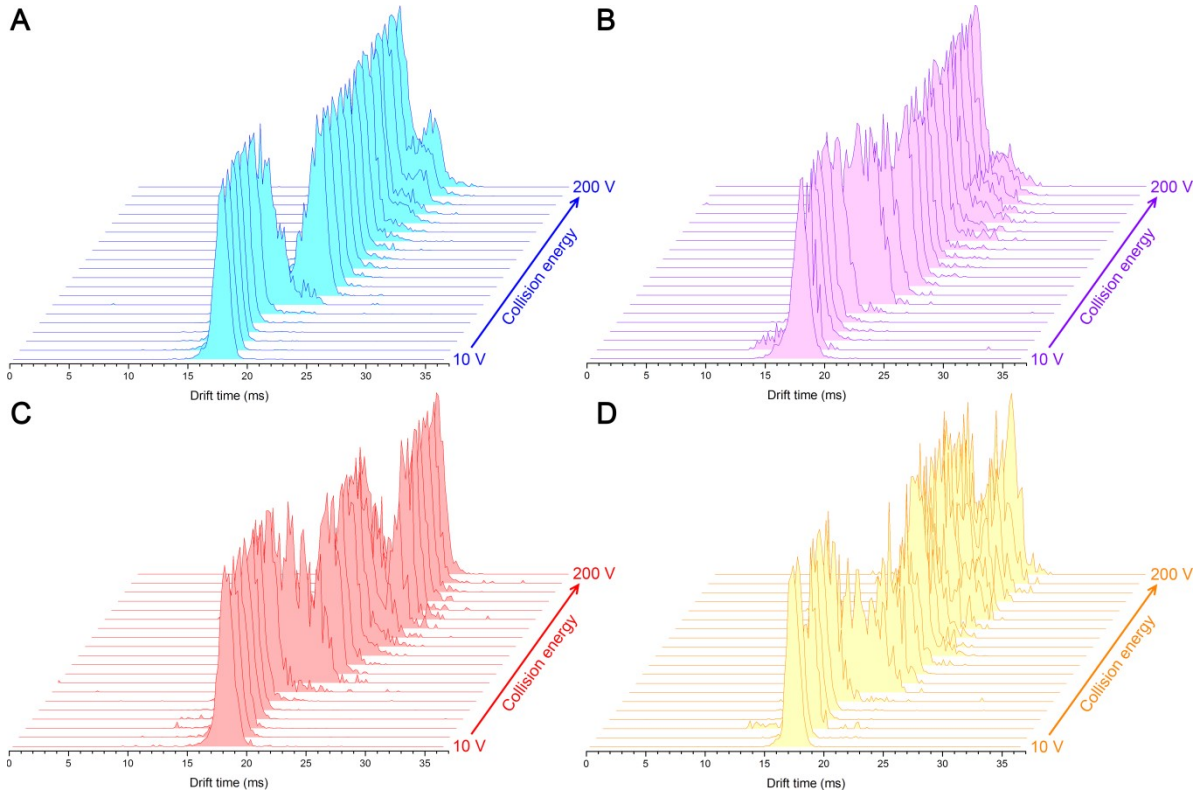

Fig. S1. IM-MS drift-time distributions of (A) IgG1κ, (B) IgG2κ, (C) IgG3κ, and (D) IgG4κ at the charge state of 21+ with collision energy ranging from 10 V to 200 V. Each IM-MS spectrum was normalized for different collision energies.

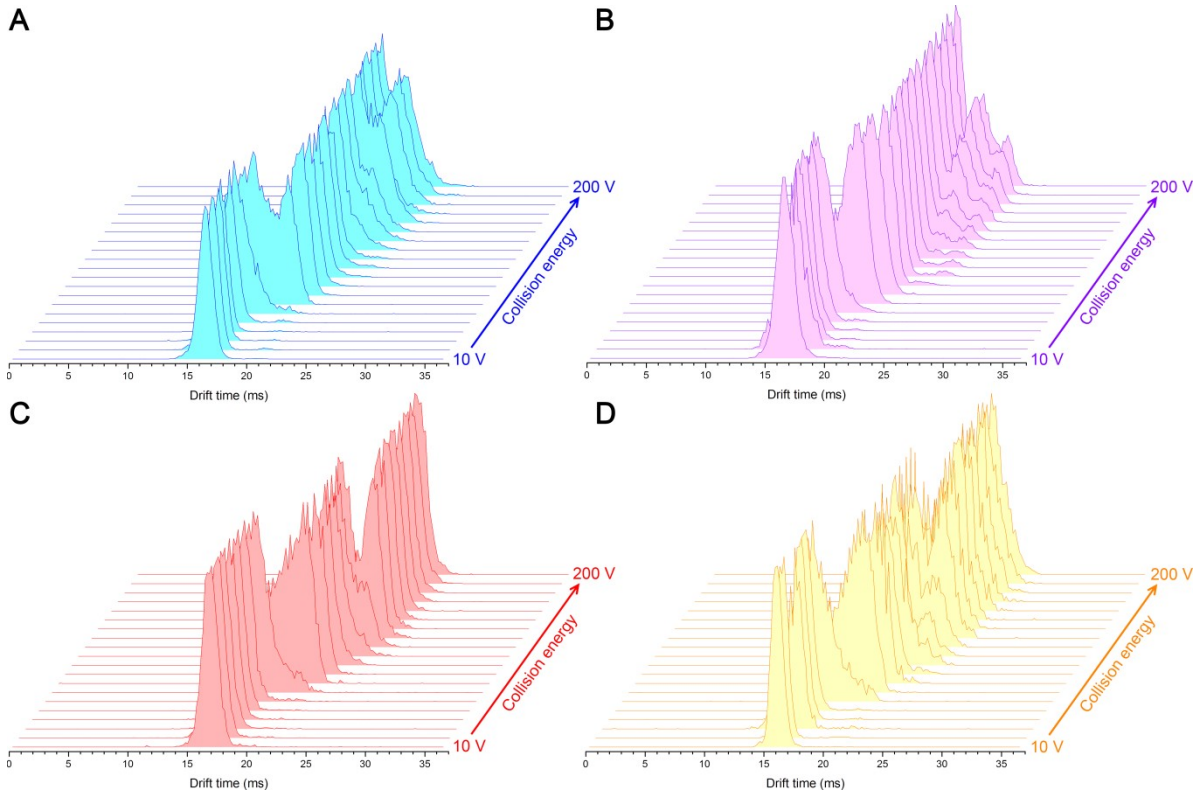

Fig. S2. IM-MS drift-time distributions of (A) IgG1κ, (B) IgG2κ, (C) IgG3κ, and (D) IgG4κ at the charge state of 22+ with collision energy ranging from 10 V to 200 V. Each IM-MS spectrum was normalized for different collision energies.

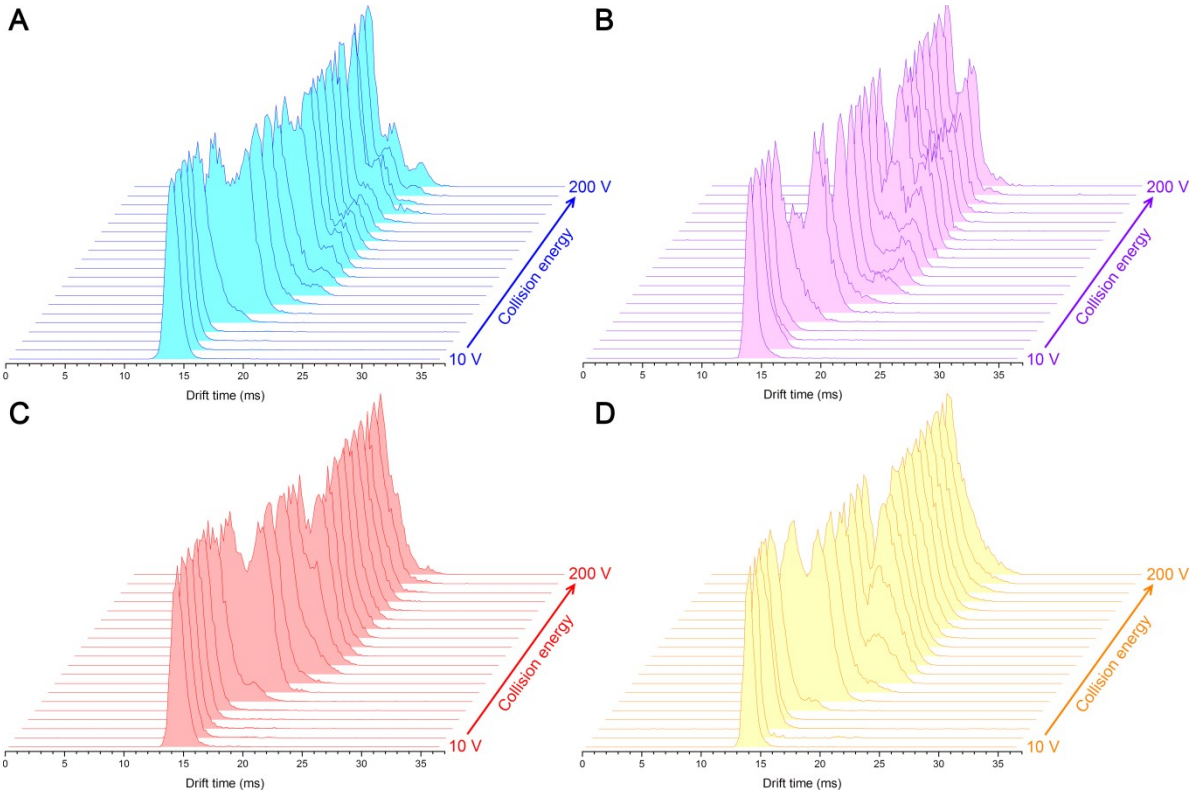

Fig. S3. IM-MS drift-time distributions of (A) IgG1κ, (B) IgG2κ, (C) IgG3κ, and (D) IgG4κ at the charge state of 24+ with collision energy ranging from 10 V to 200 V. Each IM-MS spectrum was normalized for different collision energies.

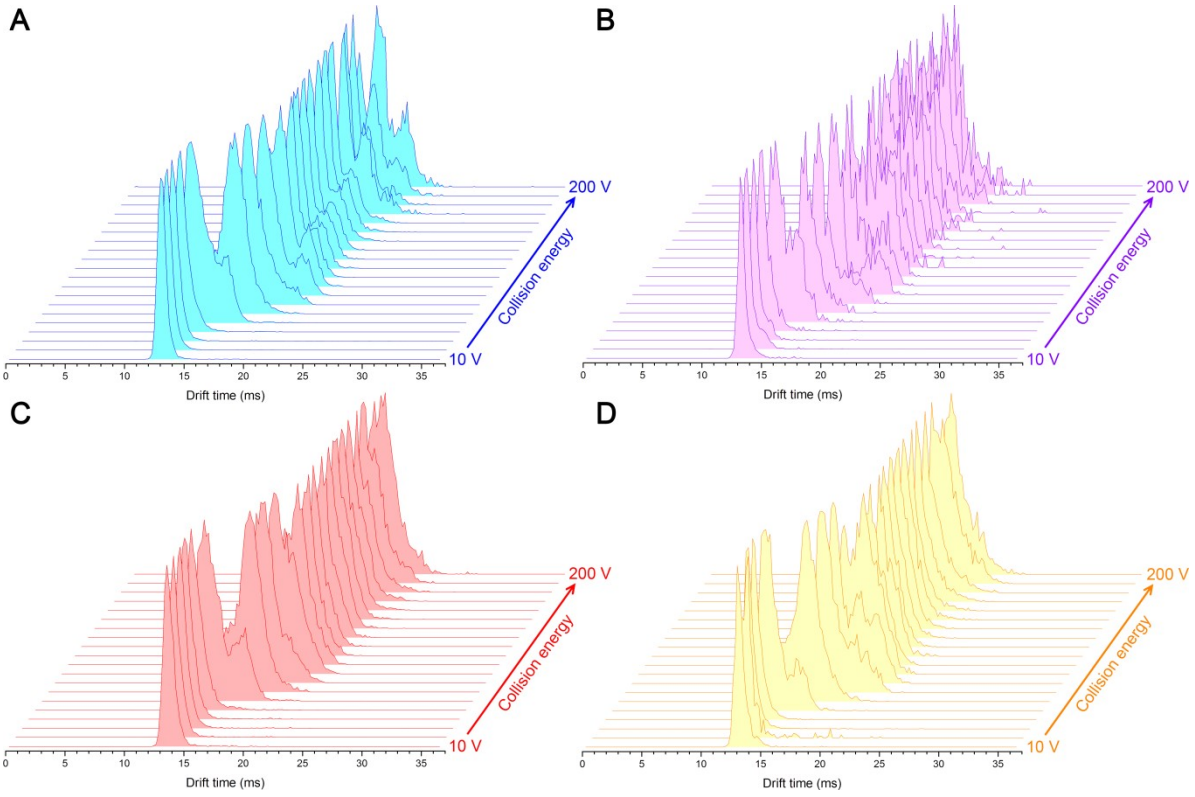

Fig. S4. IM-MS drift-time distributions of (A) IgG1κ, (B) IgG2κ, (C) IgG3κ, and (D) IgG4κ at the charge state of 25+ with collision energy ranging from 10 V to 200 V. Each IM-MS spectrum was normalized for different collision energies.

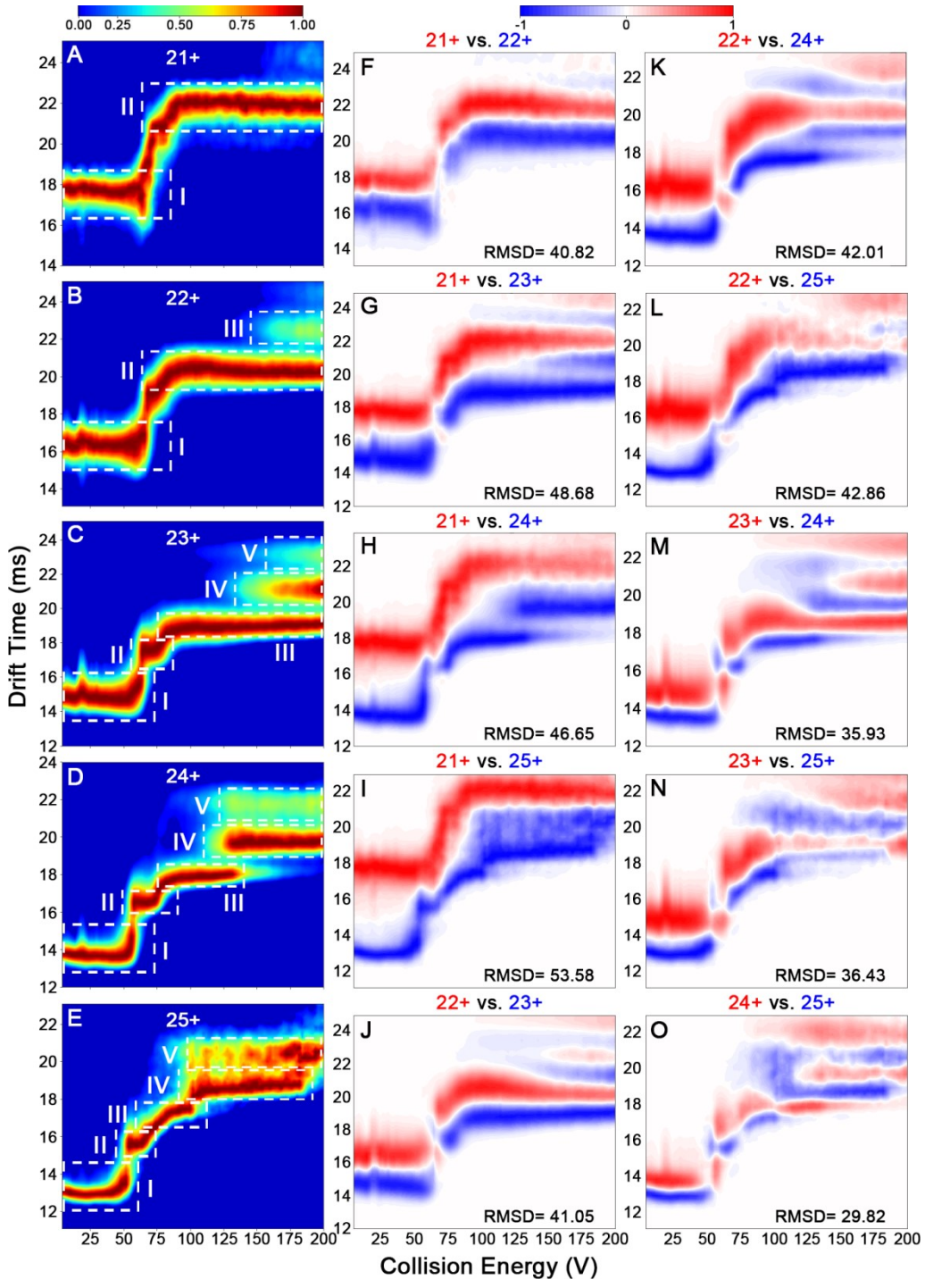

Fig. S5. CIU fingerprints of IgG2κ at the charge state of (A) 21+, (B) 22+, (C) 23+, (D) 24+, and (E) 25+. CIU difference plots of (F) 21+ vs. 22+, (G) 21+ vs. 23+, (H) 21+ vs. 24+, (I) 21+ vs. 25+, (J) 22+ vs. 23+, (K) 22+ vs. 24+, (L) 22+ vs. 25+, (M) 23+ vs. 24+, (N) 23+ vs. 25+, and (O) 24+ vs. 25+.

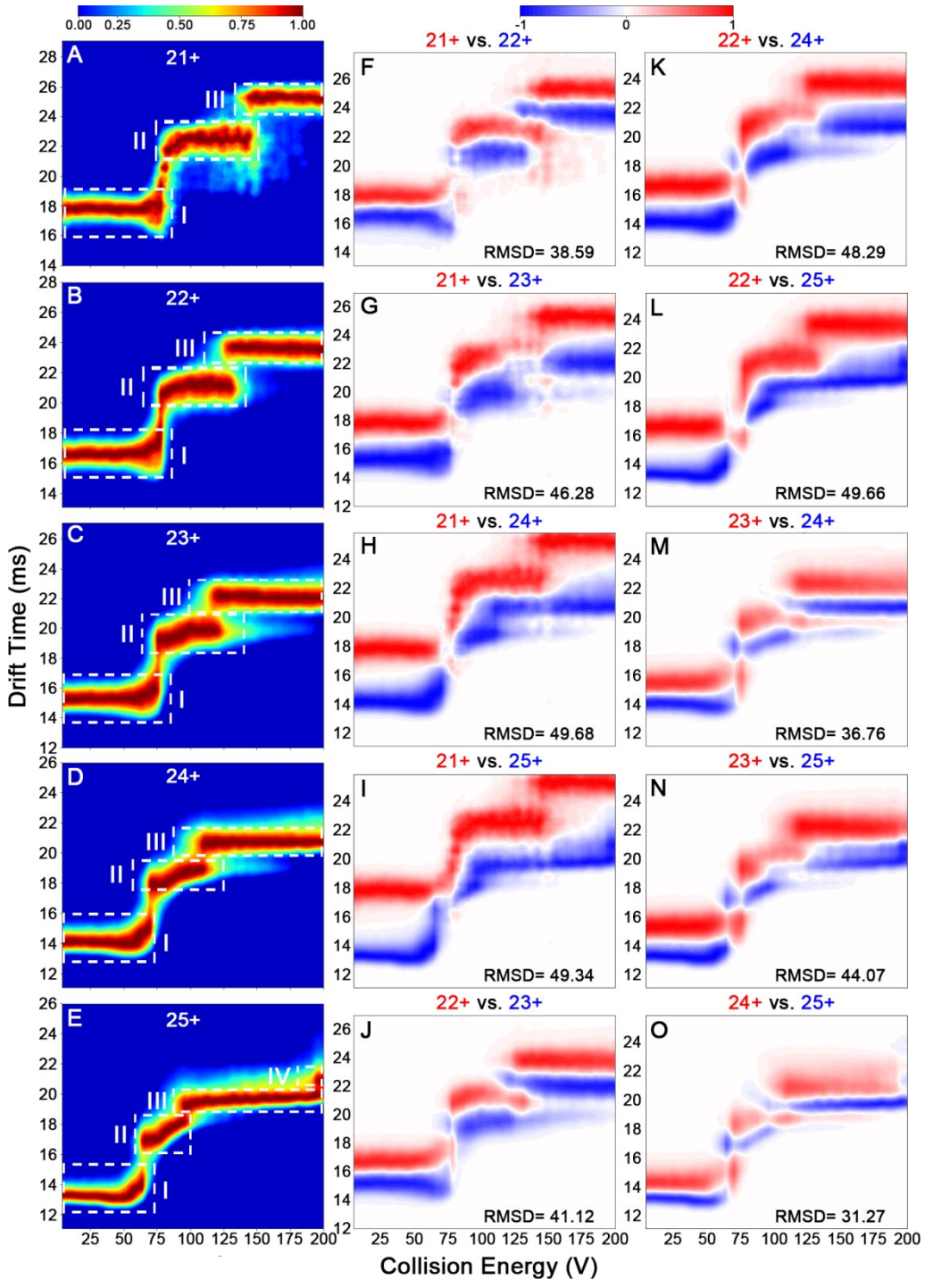

Fig. S6. CIU fingerprints of IgG3κ at the charge state of (A) 21+, (B) 22+, (C) 23+, (D) 24+, and (E) 25+. CIU difference plots of (F) 21+ vs. 22+, (G) 21+ vs. 23+, (H) 21+ vs. 24+, (I) 21+ vs. 25+, (J) 22+ vs. 23+, (K) 22+ vs. 24+, (L) 22+ vs. 25+, (M) 23+ vs. 24+, (N) 23+ vs. 25+, and (O) 24+ vs. 25+.

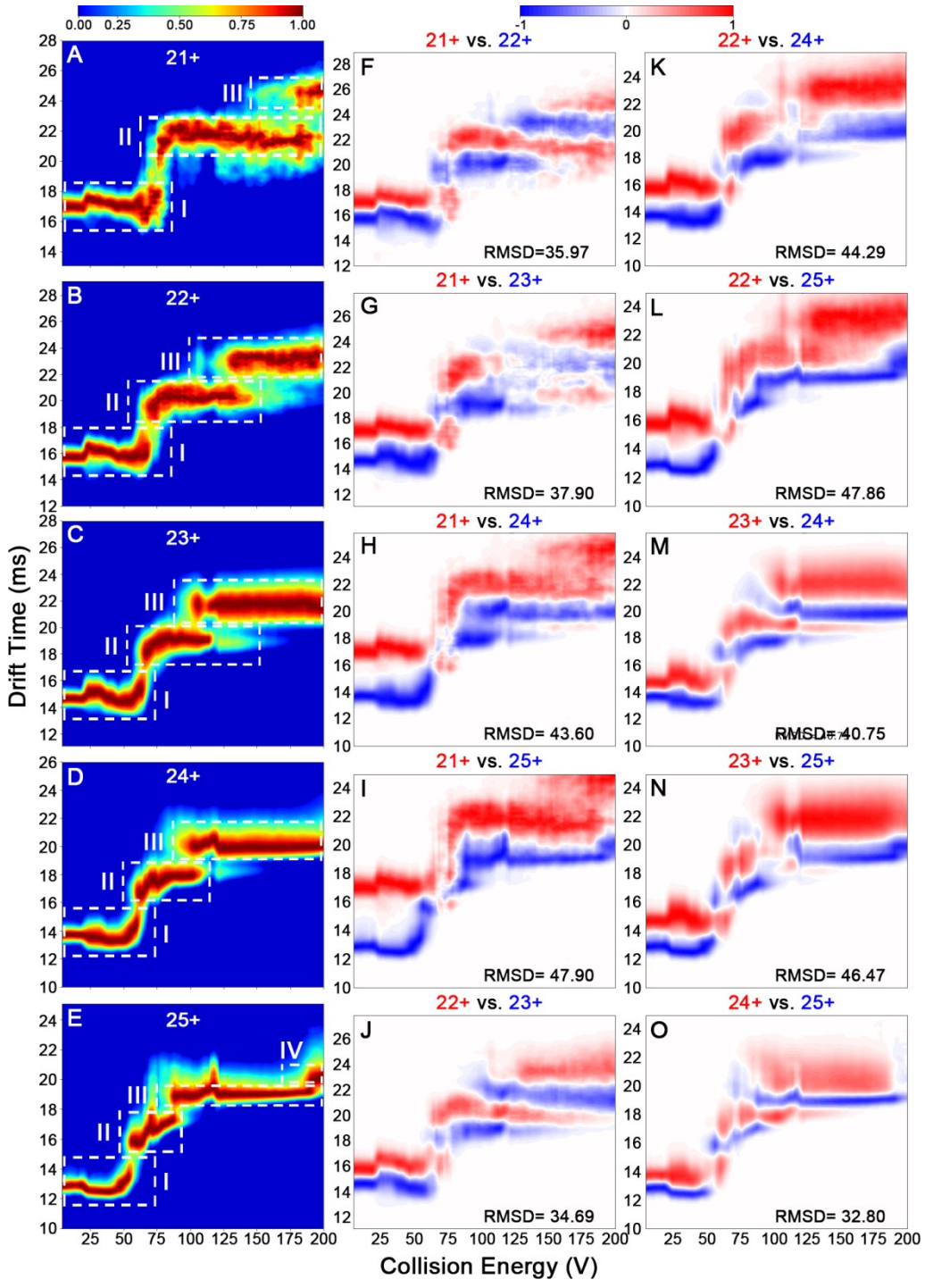

Fig. S7. CIU fingerprints of IgG4κ at the charge state of (A) 21+, (B) 22+, (C) 23+, (D) 24+, and (E) 25+. CIU difference plots of (F) 21+ vs. 22+, (G) 21+ vs. 23+, (H) 21+ vs. 24+, (I) 21+ vs. 25+, (J) 22+ vs. 23+, (K) 22+ vs. 24+, (L) 22+ vs. 25+, (M) 23+ vs. 24+, (N) 23+ vs. 25+, and (O) 24+ vs. 25+.

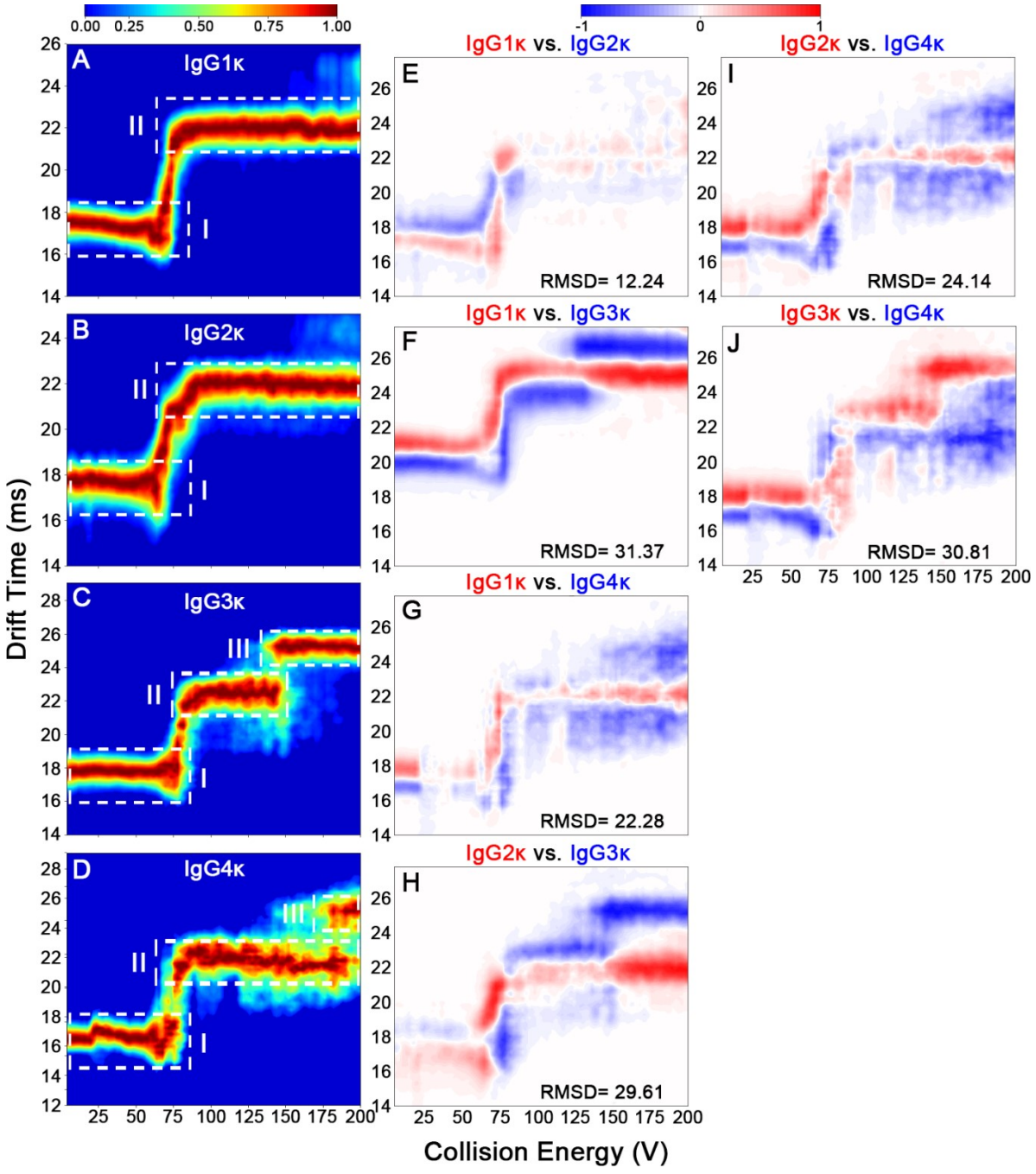

Fig. S8. CIU fingerprints of (A) IgG1κ, (B) IgG2κ, (C) IgG3κ, and (D) IgG4κ at the charge state of 21+. CIU difference plots of (E) IgG1κ vs. IgG2κ, (F) IgG1κ vs. IgG3κ, (G) IgG1κ vs. IgG4κ, (H) IgG2κ vs. IgG3κ, (I) IgG2κ vs. IgG4κ, (J) IgG3κ vs. IgG4κ.

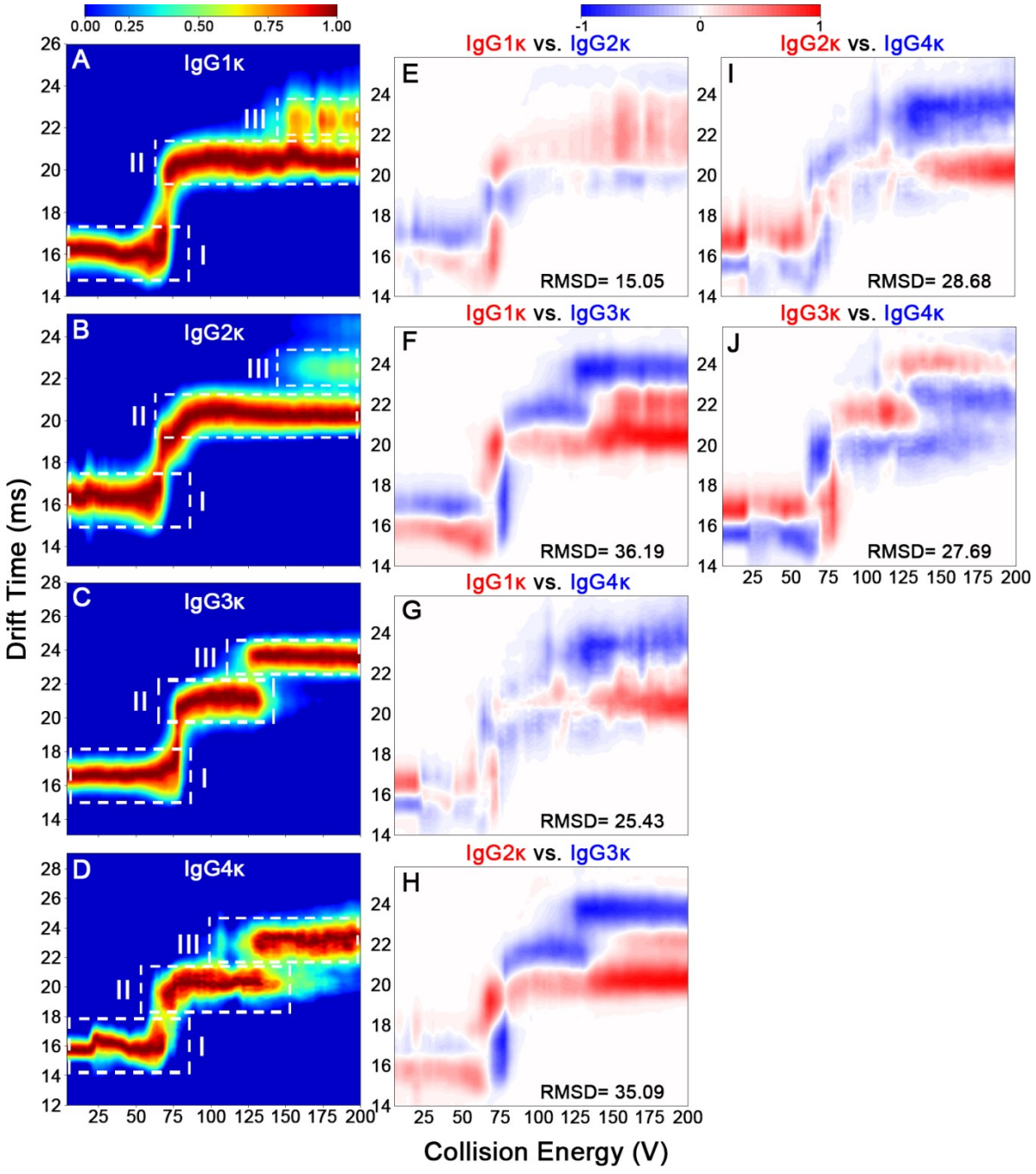

Fig. S9. CIU fingerprints of (A) IgG1κ, (B) IgG2κ, (C) IgG3κ, and (D) IgG4κ at the charge state of 22+. CIU difference plots of (E) IgG1κ vs. IgG2κ, (F) IgG1κ vs. IgG3κ, (G) IgG1κ vs. IgG4κ, (H) IgG2κ vs. IgG3κ, (I) IgG2κ vs. IgG4κ, (J) IgG3κ vs. IgG4κ.

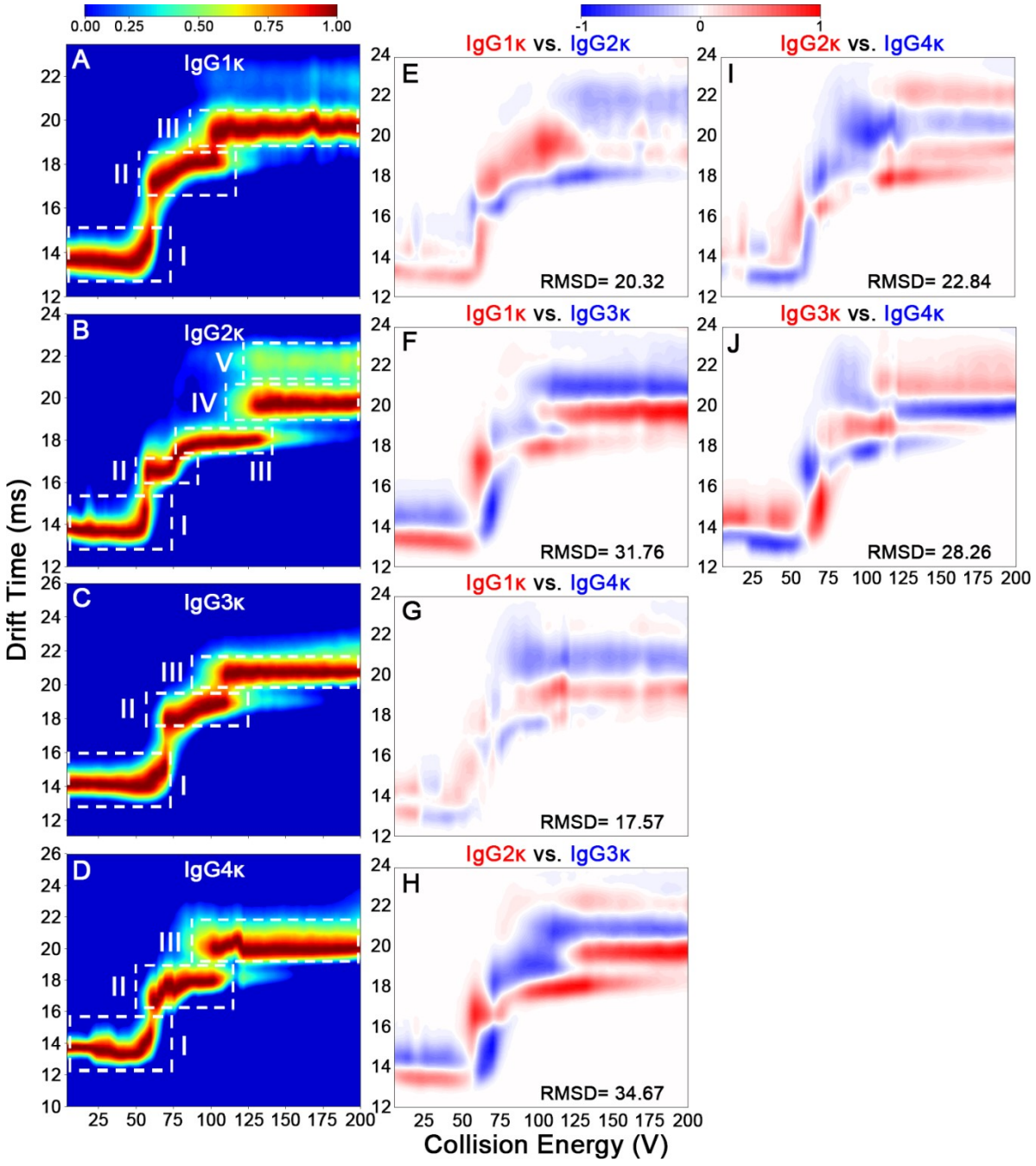

Fig. S10. CIU fingerprints of (A) IgG1κ, (B) IgG2κ, (C) IgG3κ, and (D) IgG4κ at the charge state of 24+. CIU difference plots of (E) IgG1κ vs. IgG2κ, (F) IgG1κ vs. IgG3κ, (G) IgG1κ vs. IgG4κ, (H) IgG2κ vs. IgG3κ, (I) IgG2κ vs. IgG4κ, (J) IgG3κ vs. IgG4κ.

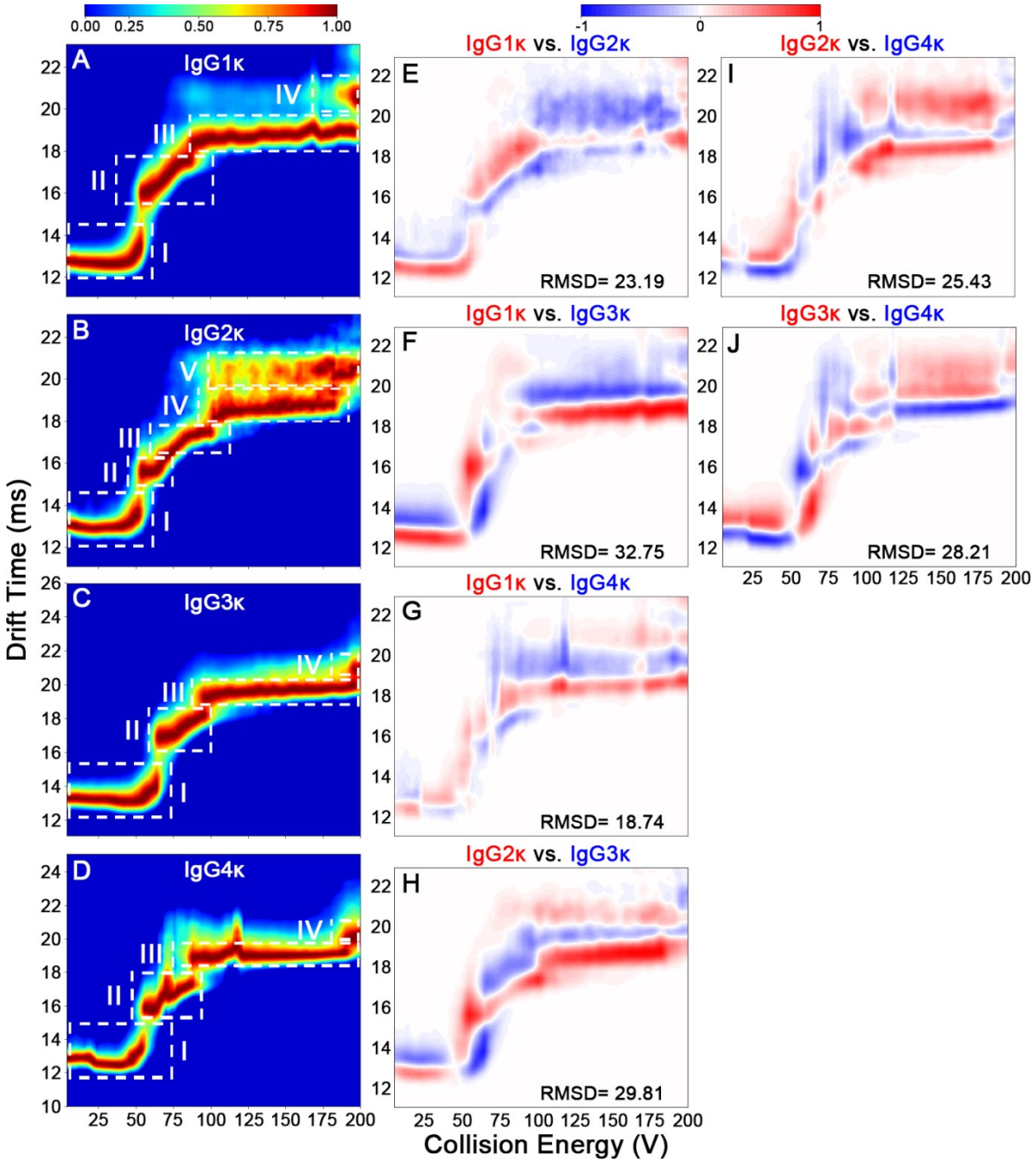

Fig. S11. CIU fingerprints of (A) IgG1κ, (B) IgG2κ, (C) IgG3κ, and (D) IgG4κ at the charge state of 25+. CIU difference plots of (E) IgG1κ vs. IgG2κ, (F) IgG1κ vs. IgG3κ, (G) IgG1κ vs. IgG4κ, (H) IgG2κ vs. IgG3κ, (I) IgG2κ vs. IgG4κ, (J) IgG3κ vs. IgG4κ.

Table S1. The detailed instrumental parameters of Synapt G2-Si HDMS

Ion source	Typical Parameter
Capillary Voltage (kV)	1.2-1.6
Sampling Cone (V)	40
Source Offset (V)	80
Temperature (°C)	30
Cone Gas (L/h)	0
Nano Flow gas (L/h)	0
Purge Gas (L/h)	0
Trap DC	
Entrance (V)	5.0
Bias (V)	50.0
Trap DC (V)	-2.0
Exit (V)	20.0
IMS	
Entrance (V)	10.0
Helium Cell DC (V)	50.0
Helium Exit (V)	-40.0
Bias (V)	3.0
Exit (V)	2.0
Transfer DC	
Entrance (V)	15.0
Exit (V)	15.0
TriWave	
Wave Velocity (m/s)	250.0
Wave Height (V)	2.0
IMS	

Wave Velocity (m/s)	600.0
Wave Height (V)	40.0
Transfer	
Wave Velocity (m/s)	175.0
Wave Height (V)	12.0
StepWave 1	
Wave Velocity (m/s)	300.0
Wave Height (V)	10.0
StepWave 2	
Wave Velocity (m/s)	300.0
Wave Height (V)	0.0
StepWave DC	
StepWave 2 Offset	60.0
Diff Aperture 1	10.0
Diff Aperture 2	10.0
Source Ion Guide	
Wave Velocity (m/s)	300.0
Wave Height (V)	0.0
RF Setting	
StepWave (V)	300.0
Ion Source (V)	350.0
Gas Control	
Trap (V)	2.0
Helium Cell (L/h)	200.0
IMS (V)	80.0
MS Profile Type	Auto Profile
Mass 1	1.25 Ma (Low m/z limit)
Dwell Time 1	25%

Ramp Time 1	75%
Mass 2	0.17 Mb (High *m/z* limit)

Table S2. The transition voltage required for conformation transition.

	21+	22+	23+	24+	25+
IgG1κ	73.8 V	68.5 V	66.5 V	60.4 V	54.4 V
		145.0	134.5 V	103.3 V	82.5 V
					168.5 V
IgG2κ	69.7 V	66.8 V	62.6 V	56.4 V	52.7 V
		155.1 V	74.9 V	74.2 V	72.1 V
			132.5 V	114.5 V	101.7 V
			163.2 V	120.0 V	97.6 V
IgG3κ	77.9 V	76.9 V	74.9 V	70.6 V	64.8 V
	136.0 V	122.4 V	110.2 V	94.8 V	83.1 V
					169.8 V
IgG4κ	76.8 V	65.1 V	62.5 V	57.5 V	54.5 V
	150.1 V	123.8 V	92.2 V	87.5 V	82.1 V
					179.3 V

Table S3. RMSD values acquired from IgG subtypes with different charge states.

	21+	22+	23+	24+	25+
IgG1κ vs. IgG2κ	12.24	15.05	19.45	20.32	23.19
IgG1κ vs. IgG3κ	31.37	36.19	34.73	31.76	32.75
IgG1κ vs. IgG4κ	22.28	25.43	28.67	17.57	18.74
IgG2κ vs. IgG3κ	29.61	35.09	37.05	34.67	29.81
IgG2κ vs. IgG4κ	24.14	28.68	32.34	22.84	25.43
IgG3κ vs. IgG4κ	30.81	27.69	25.74	28.26	28.21